GROUND DATA PROCESSING & PRODUCTION OF THE LEVEL 1 HIGH RESOLUTION MAPS

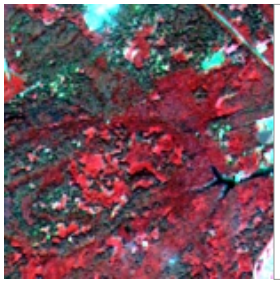

VALERI 2004

Sonian forest site
(forest)

Philippe Rossello

June 2006

CONTENTS

1. Introduction

This report describes the production of the high resolution, level 1, biophysical variable maps for the Sonian forest site in 2004. Level 1 map corresponds to the map derived from the determination of a transfer function between reflectance values of the SPOT image acquired during (or around) the ground campaign, and biophysical variable measurements (hemispherical images). For each Elementary Sampling Unit (ESU), the hemispherical images were processed using the CAN-EYE software (Version 3.5) developed at INRA-CSE. The derived biophysical variable maps are:

• four Leaf Area Index (LAI) are considered: effective LAI (LAIeff) and true LAI (LAItrue) derived from the description of the gap fraction as a function of the view zenith angle; effective LAI57 (LAI57eff) and true LAI57 (LAI57true) derived from the gap fraction at 57.5°, which is independent on the leaf inclination. Effective LAI and effective LAI57 do not take into account clumping effect. LAItrue and LAI57true are derived using the method proposed by Lang and Yueqin[1] (1986);

• cover fraction (fCover): it is the percentage of soil covered by vegetation. To improve the spatial sampling, fCover was computed over 0 to 10° zenith angle;

• fAPAR: it is the fraction of Absorbed Photosynthetically Active Radiation (PAR=400-700nm). The fAPAR is defined either instantaneously (for a given solar position) or integrated all over the day. Following a study based on radiative transfer model simulations, it has been shown that the root mean square error between instantaneous fAPAR computed every 30 minutes and the daily fAPAR is the lowest for instantaneous fAPAR at 10h00 AM (solar time, RMSE = 0.021). Therefore, the derivation of fAPAR from CAN-EYE corresponds to the instantaneous black sky fAPAR at 10h00 AM.

The land cover is mainly composed of forests (beeches, oaks, chestnut trees…). Note that the underwood is sometimes very dense (ferns, grass…).

The site coordinates are described in Table 1:

	UTM 31, North, WGS-84 (units = meters)		Geographic Lat/Lon WGS-84 (units = degrees)	
	Easting	Northing	Lat.	Lon.
Upper left corner	597985.6240	5626512.0830	50.78207463	4.38993775
Lower right corner	601025.6240	5623472.0830	50.75422317	4.43221148
Center	599505.6240	5624992.0830	50.76815078	4.41108089

Table 1. Description of the site coordinates: they correspond to SPOT image coordinates.

2. Available data

2.1. SPOT Image

The SPOT image was acquired the 28th July 2004 by HRVIR1 on SPOT4 while the ground measurements were carried out from 21/06/2004 to 22/06/2004. It was geo-located by SPOT image (SPOTView, precision 2B). The projection is UTM 31 North, WGS-84. No atmospheric correction was applied to the image since no atmospheric data were available. However, as the SPOT image is used to compute empirical relationships between reflectance and biophysical variable, we can assume that the effect of the atmosphere is the same over the whole 3 x 3 km site. Therefore, it will be taken into account everywhere in the same way.

Figure 1 shows the relationship between Red and near infrared (NIR) SPOT channels: the soil line is rather marked and no saturated points are observed.

[1] Lang, A.R.G. and Yueqin, X., 1986. Estimation of leaf area index from transmission of direct sunlight in discontinuous canopies. Agric. For. Meteorol., 37: 229-243.

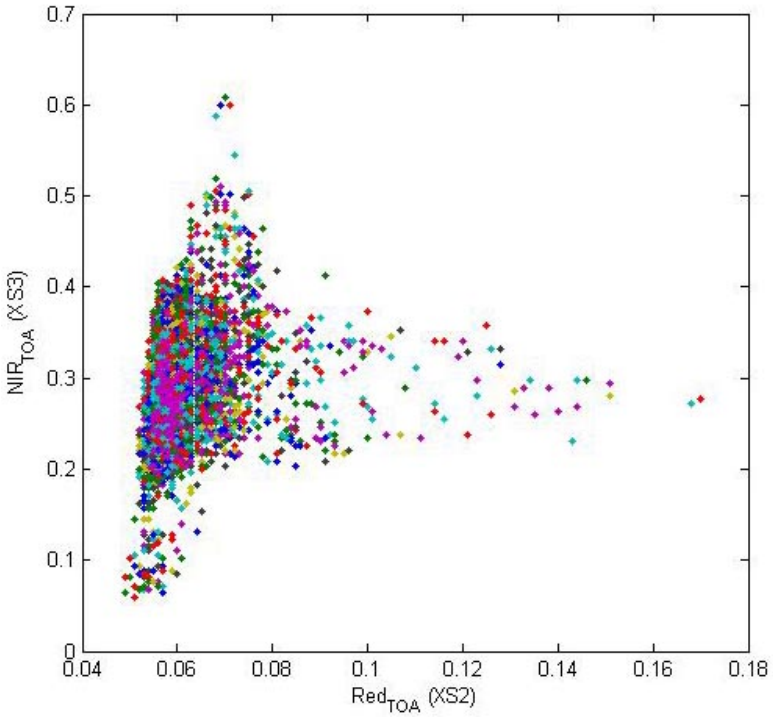

Figure 1. Red/NIR relationship on the SPOT image for Sonian forest, 2004.

2.2. Hemispherical images

The hemispherical images were processed using the CAN-EYE software (Version 3.5) to derive the biophysical variables.

Figure 2 and Figure 3 show the distribution of the several variables over the 38 sampled ESUs. As there was understorey on all the ESUs[2], hemispherical images were acquired from above the understorey and from below the canopy (trees). The two sets of acquisition were processed separately to derived LAI (effective and true), LAI57 (effective and true), fCover, and fAPAR. The ESU biophysical variable was then computed as:

- LAIeff, LAI57eff, LAItrue, LAI57true: LAI(above) + LAI(below).
- fCover: 1-(1-fCover(above))*(1-fCover(below)). This assumes that independency of the gaps inside the understorey and the gaps inside the trees which is not true at all the scales but it is the only way to get the total fCover. However, for the local scales considered, this might be true as a first order approximation.
- fAPAR: [1-(1-fAPAR(below))*(1-fAPAR(above))], since 1-fAPAR can be considered equivalent to a gap fraction. Here again, the same independency between the two layers has to be assumed.

Note that LAI (effective and true) derived from directional gap fraction and LAI derived from gap fraction at 57.5° (effective and true) are consistent (Figure 2 and Figure 3). Effective LAI (LAIeff, LAI57eff) varies from 1.24 to 5.6, while true LAI (LAItrue, LAI57true) varies from 2.36 to 9.97 (E13, E16, E02 and E06 > 7). This range shows a quite heterogeneous site in terms of LAI. For values, LAIeff and LAI57eff are lower than LAItrue and LAI57true. This is due to the clumping observed for several ESUs. The relationship between fAPAR and LAI is in agreement with what is expected (Beer-Lambert law) while the fCover-LAI relationship is more noisy.

To build the relationships between biophysical variables and SPOT data, the reflectance of a given forest ESU was considered as the average reflectance over the central pixel + the 8 surrounding pixels. This takes into account the fact that the height of the trees are about 20 m and consequently the fish-eye observes an area of $\pi \times [20 \times \tan(60°)]^2 \cong 3800$ m², *i.e.* close to the area of 9 SPOT pixels (=3600m²) when using a maximum view zenith angle of 60°.

[2] except E22: the images acquired from above the understorey were fuzzy.

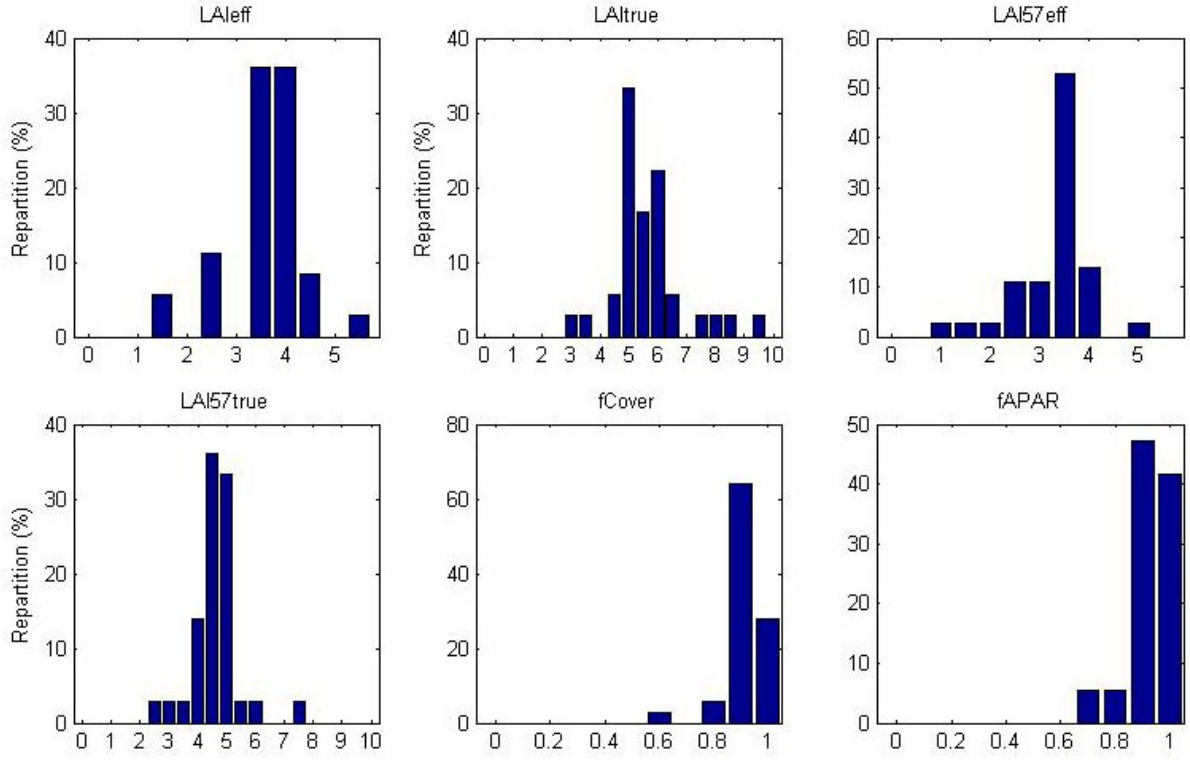

Figure 2. Distribution of the measured biophysical variables over the ESUs.

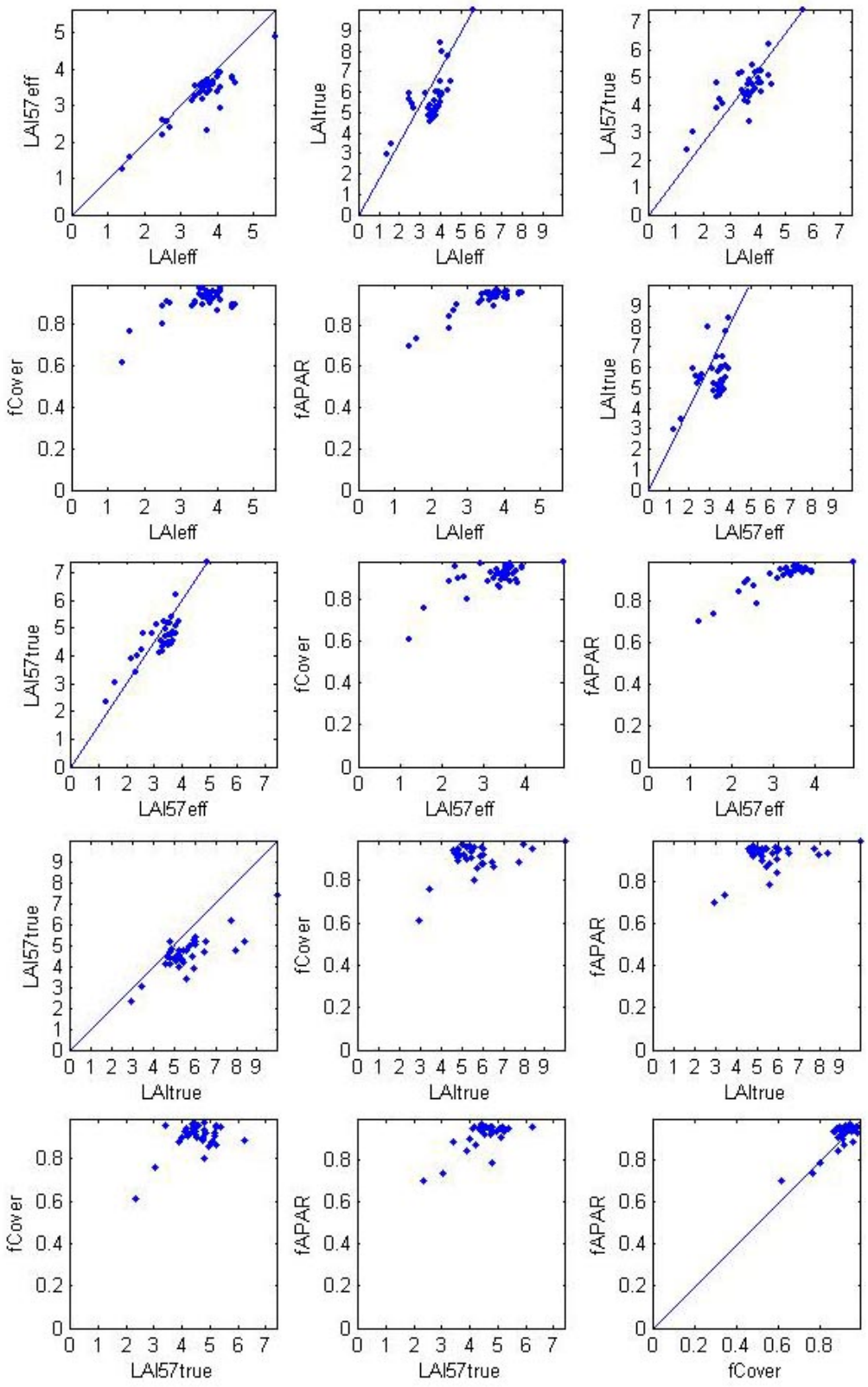

Figure 3. Relationships between the different biophysical variables

2.3. Sampling strategy

2.3.1. Principles

The sampling of each ESU is based on twelve elementary photographs. Figure 4 shows that the 38 ESUs are evenly distributed over the site (3 x 3 km). The processing of the ground data has shown that:

• E04 (in black on Figure 5) was located on a small plot with a strong heterogeneity: it has been eliminated;
• E10 (in black on Figure 5) was also eliminated because it is geo-located under a cloud. The reflectance value is thus wrong. Note that the cloud pixels were identified (a default value has been attributed). The transfer function does not take them into account.

Finally the 36 ESUs have been kept for the computation of the transfer function.

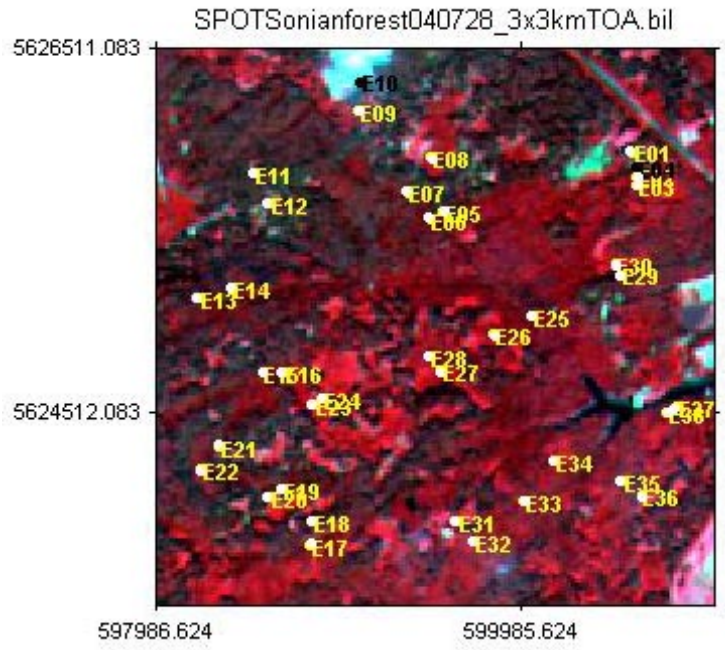

Figure 4. Distribution of the ESUs around the Sonian forest site.
ESUs in black (E04, E10) were eliminated for the computation of the transfer function.

2.3.2. Evaluation based on NDVI values

The sampling strategy is evaluated using the SPOT image by comparing the NDVI distribution over the site with the NDVI distribution over the ESUs (Figure 5). As the number of pixels is drastically different for the ESU and whole site (WS = 22500 in case of a 3 x 3 km SPOT image at 20 m resolution), it is not statistically consistent to directly compare the two NDVI histograms. Therefore, the proposed technique consists in comparing the NDVI cumulative frequency of the two distributions by a Monte-Carlo procedure which aims at comparing the actual frequency to randomly shifted sampling patterns. It consists in:

1. computing the cumulative frequency of the N pixel NDVI that correspond to the exact ESU locations;
2. then, applying a unique random translation to the sampling design (modulo the size of the image);
3. computing the cumulative frequency of NDVI on the randomly shifted sampling design;
4. repeating steps 2 and 3, 199 times with 199 different random translation vectors.

This provides a total population of $N = 199 + 1$(actual) cumulative frequency on which a statistical test at acceptance probability $1 - \alpha = 95\%$ is applied: for a given NDVI level, if the actual ESU density function is between two limits defined by the $N\alpha/2 = 5$ highest and lowest values of the 200 cumulative frequencies, the hypothesis assuming that WS and ESU NDVI distributions are equivalent is accepted, otherwise it is rejected.

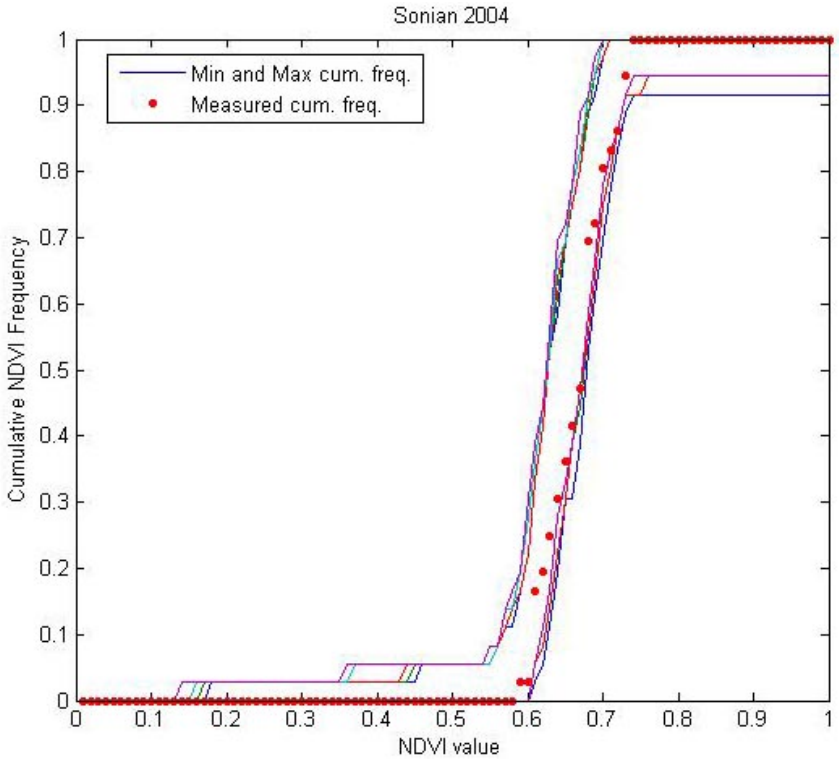

Figure 5. Comparison of the ESU NDVI distribution and the NDVI distribution over the whole image.

Figure 5 shows that the NDVI distribution of the 36 ESUs is good over the whole site even if the cumulative frequency curve is very close to the boundaries for NDVI values comprised between 0.64 and 0.73. Note that NDVIs lower than 0.59 have not been sampled although they are present in the image. The site is quite homogeneous in terms of NDVI since the highest and lowest distributions are close.

2.3.3. Evaluation based on classification

A non supervised classification based on the k_means method (Matlab statistics toolbox) was applied to the reflectance of the SPOT image to distinguish if different behaviours on the image for the biophysical variable-reflectance relationship exist.

A number of 5 classes was chosen (Figure 6). The distribution of the classes on the image and on the ESUs is quite similar: class 2 is equivalent, class 1 appears to be over-sampled while classes 4 and 5 are under-represented. The class 3 is not represented because E10 was eliminated. It corresponds to cloud class.

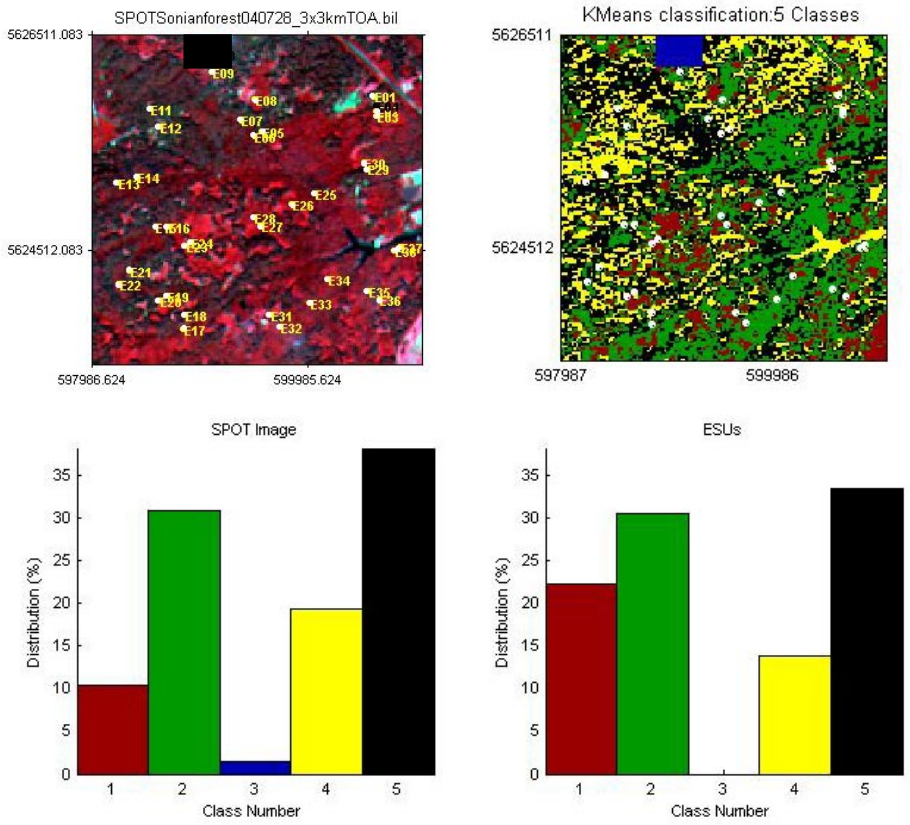

Figure 6. Classification of the SPOT image. Comparison of the class distribution between the SPOT image and sampled ESUs. In rend

Figure 7 shows the different relationships observed between the biophysical variables and the corresponding NDVI on the ESUs, as a function of the SPOT classes determined from non supervised classification:

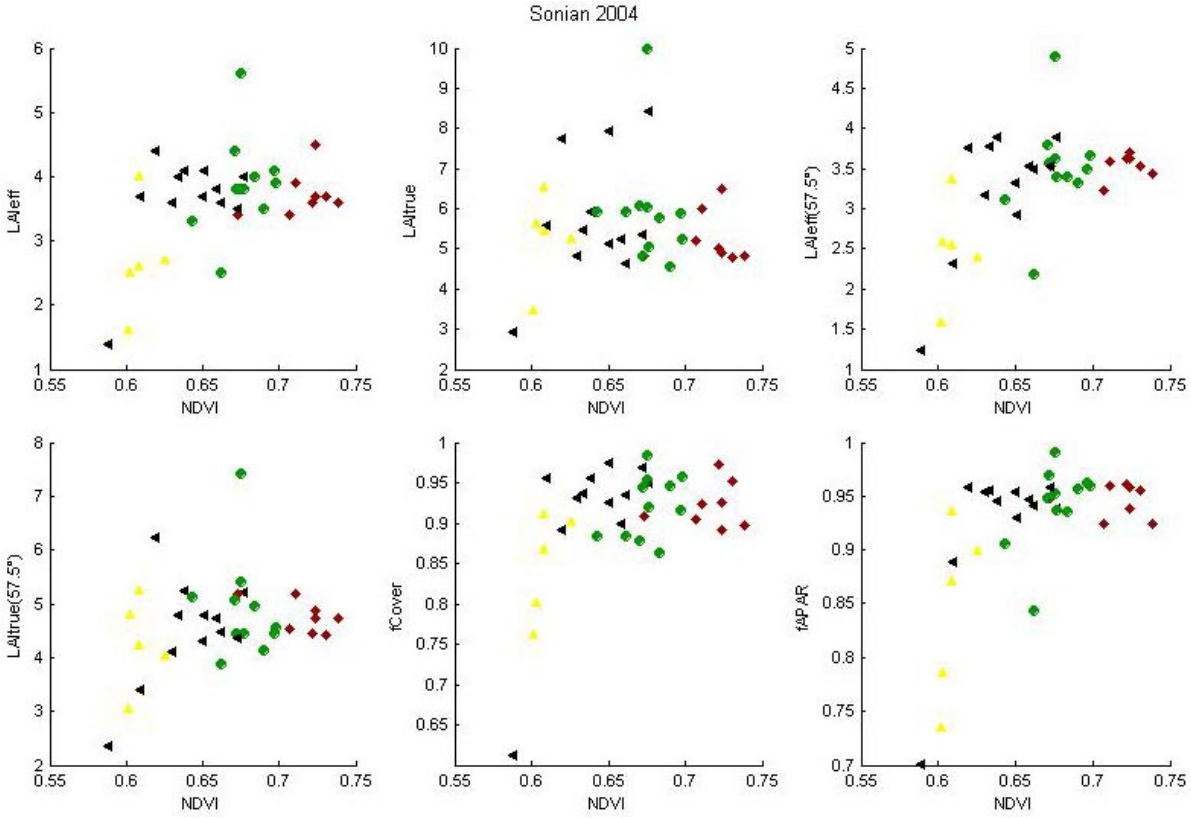

Figure 7. NDVI-Biophysical Variable relationships as a function of SPOT classes

The relation between NDVI and biophysical variables is not significant. The biophysical variable values are relatively homogeneous even if a few biophysical variable values are very slight compared with NDVI values or conversely. For example, the LAI is very slight for E12 (sparse beeches, ferns, brambles) and E19 (forest cut with tall beeches, ferns, brambles) while NDVI values are relatively high. The highest biophysical variable values correspond to ESUs having strong tree density and dense underwood. Note that the minimum NDVI value is very high (0.58).

Therefore, a single transfer function per variable will be generated. A default value will be attributed to the pixels corresponding to the cloud.

2.3.4. Using convex hulls

A test based on the convex hulls was also carried out to characterize the representativeness of ESUs. Whereas the evaluation based on NDVI values uses two bands (red and NIR), this test uses the four bands of the SPOT image. A flag image, is computing over the reflectances (Figure 8). The result on convex-hulls can be interpreted as:

- pixels inside the 'strict convex-hull': a convex-hull is computed using all the SPOT reflectance corresponding to the ESUs belonging to the class. These pixels are well represented by the ground sampling and therefore, when applying a transfer function the degree of confidence in the results will be quite high, since the transfer function will be used as an interpolator;
- pixels inside the 'large convex-hull': a convex-hull is computed using all the reflectance combination (±5% in relative value) corresponding to the ESUs. For these pixels, the degree of confidence in the obtained results will be quite good, since the transfer function is used as an extrapolator (but not far from interpolator);
- pixels outside the two convex-hulls: this means that for these pixels, the transfer function will behave as an extrapolator which makes the results less reliable. However, having a priori information on the site may help to evaluate the extrapolation capacities of the transfer function.

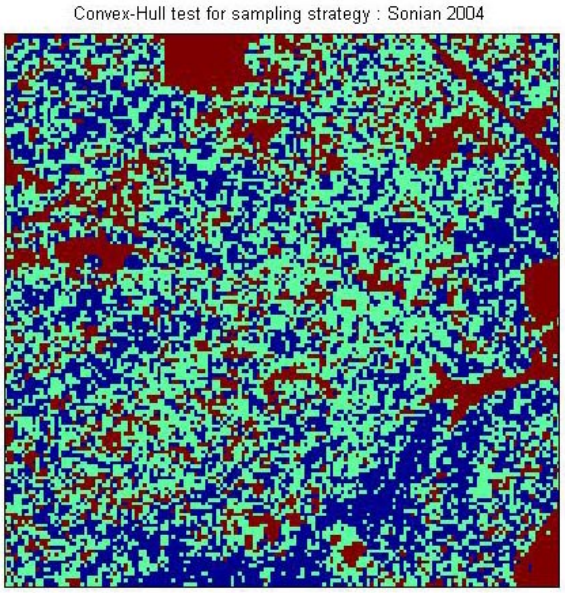

Figure 8. Evaluation of the sampling based on the convex hulls. The map is shown at the bottom: blue and light blue correspond to the pixels belonging to the 'strict' and 'large' convex hulls and red to the pixels for which the transfer function is extrapolating.

This map shows that the representativeness of the ESUs is good, even if pixels are outside the two convex-hulls. They mainly correspond to cloud, water, bare soil…

3. Determination of the transfer function for the 6 biophysical variables: LAIeff, LAI57eff, LAItrue, LAI57true, fCover, fAPAR

3.1. The transfer function considered

For each class determined in §2.3, the following transfer functions were tested:

- AVE: if the number of ESUs belonging to the class is too low. The transfer function consists only in attributing the average value of the biophysical variable measured on the class to each pixel of the SPOT image belonging to the class;

- REG: if the number of ESUs is sufficient, multiple robust regression between ESUs reflectance (or Simple Ratio) and the considered biophysical variable can be applied: we used the 'robustfit' function from the Matlab statistics toolbox. It uses an iteratively re-weighted least squares algorithm, with the weights at each iteration computed by applying the bisquare function to the residuals from the previous iteration. This algorithm provides lower weight to ESUs that do not fit well. The results are less sensitive to outliers in the data as compared with ordinary least squares regression. At the end of the processing, three errors are computed: classical root mean square error (RMSE), weighted RMSE (using the weights attributed to each ESU) and cross-validation RMSE (leave-one-out method).

Although there is no evident relationship between NDVI and LAI (§2.3.3), we tested the multiple robust regression (REG) which did not show pertinent results, even if a middle infrared band was available. Therefore, even if the number of ESUs belonging to the classes is sufficient, the 'AVE' method is applied. For each class determined in §2.3 (classes 1, 2, 4 and 5), the transfer function consists only in attributing the average value of the biophysical variable measured on the class to each pixel of the SPOT image belonging to the class.

3.2. Results

Following, the results of the transfer function:

	LAIeff	LAItrue	LAI57eff	LAI57true	fCover	fAPAR
Class 1	3.725	5.255	3.5313	4.7563	0.9217	0.94622
Class 2	3.8818	5.9318	3.4955	4.9009	0.92101	0.94197
Class 3 (cloud)	*-0.001*	*-0.001*	*-0.001*	*-0.001*	*-0.001*	*-0.001*
Class 4	2.68	5.254	2.496	4.254	0.84839	0.84524
Class 5	3.6583	5.765	3.24	4.4975	0.91147	0.92265

Table 2. Transfer function applied to the whole site for the different biophysical variables

The values of biophysical variable maps are homogeneous with close values between class 1, class 2 and class 5. The class 3 values correspond to cloud: a default value (-0.001) is attributed to the pixels belonging to this class. The class 4 values are lower. The pixels correspond to sparse beeches, ferns, chestnut trees…

Note that the average value of the ESUs values per biophysical variable over the whole Sonian forest site is also representative (except class 4): LAIeff.ESU = 3.605; LAItrue.ESU = 5.631; LAI57eff.ESU = 3.279; LAI57true.ESU = 4.644; fCover.ESU = 0.907; fAPAR.ESU = 0.923.

4. Conclusion

The transfer function is obtained by using 36 ESUs. The values of biophysical variable maps are quite homogeneous (except class 4 which is heterogeneous: sparse beeches, ferns, chestnut trees, brambles…). Note that no relationship exists between LAI and NDVI, as well as biophysical variable and SPOT reflectances. When the canopy is dense, the underwood evaluation from the reflectance is probably not very reliable. Therefore, the selected transfer function consists in attributing the average value of the biophysical variable measured on the class to each pixel of the SPOT image belonging to the class. The average value of the ESUs per biophysical variable over the whole site is also representative (except class 4) and consistent with the obtained maps (§3.2).

The biophysical variable maps are available in UTM, 31 North, projection coordinates (Datum: WGS-84) at 20m resolution.

5. Acknowledgements

We want to thank: **Piet Boekaerts** (VUB/ETRO-IRIS, Brussel), **Frédéric Baret** (INRA-CSE, Avignon), but also **Sandrine** and **Peter** for the organisation and participation to the campaign.